5-16-2017

Ozone and haze pollution weakens net primary productivity in China

Xu Yue
Chinese Academy of Sciences

Nadine Unger
University of Exeter

Kandice Harper
Yale University

Xiangao Xia
Chinese Academy of Sciences

Hong Liao
Nanjing University of Information Science & Technology

See next page for additional authors

Comments

This is an article published by European Geosciences Union in Atmospheric Chemistry and Physics in 2017, available online: https://dx.doi.org/10.5194/acp-17-6073-2017

Recommended Citation

Yue, X., Unger, N., Harper, K., Xia, X., Liao, H., Zhu, T., Xiao, J., Feng, Z., Li, J. (2017). Ozone and haze pollution weakens net primary productivity in China. Atmospheric Chemistry and Physics, 17, 6073-6089. (Journal Highlight Article). https://dx.doi.org/10.5194/acp-17-6073-2017

Authors
Xu Yue, Nadine Unger, Kandice Harper, Xiangao Xia, Hong Liao, Tong Zhu, Jingfeng Xiao, Zhaozhong Feng, and Jing Li

AGU PUBLICATIONS

Global Biogeochemical Cycles

RESEARCH ARTICLE

10.1002/2016GB005557

Key Points:
- Woody residence time (τ_w, years) is related to forest age, annual temperature, and precipitation
- Influences of meteorological drivers on τ_w are different among various plant functional types
- The estimated global forest τ_w shows large spatial heterogeneity, and this strongly influences model simulation of AGB

Supporting Information:
- Supporting Information S1

Correspondence to:
Q. Guo,
guo.qinghua@gmail.com

Citation:
Xue, B.-L., Q. Guo, T. Hu, J. Xiao, Y. Yang, G. Wang, S. Tao, Y. Su, J. Liu, and X. Zhao (2017), Global patterns of woody residence time and its influence on model simulation of aboveground biomass, *Global Biogeochem. Cycles*, *31*, 821–835, doi:10.1002/2016GB005557.

Received 17 OCT 2016
Accepted 19 APR 2017
Accepted article online 23 APR 2017
Published online 13 MAY 2017

Global patterns of woody residence time and its influence on model simulation of aboveground biomass

Bao-Lin Xue[1], Qinghua Guo[1,2], Tianyu Hu[1], Jingfeng Xiao[3], Yuanhe Yang[1], Guoqiang Wang[4], Shengli Tao[1], Yanjun Su[2], Jin Liu[1], and Xiaoqian Zhao[1]

[1]State Key Laboratory of Vegetation and Environmental Change, Institute of Botany, Chinese Academy of Sciences, Beijing, China, [2]School of Engineering, Sierra Nevada Research Institute, University of California, Merced, California, USA, [3]Earth Systems Research Center, Institute for the Study of Earth, Oceans, and Space, University of New Hampshire, Durham, New Hampshire, USA, [4]College of Water Sciences, Beijing Normal University, Beijing, China

Abstract Woody residence time (τ_w) is an important parameter that expresses the balance between mature forest recruitment/growth and mortality. Using field data collected from the literature, this study explored the global forest τ_w and investigated its influence on model simulations of aboveground biomass (AGB) at a global scale. Specifically, τ_w was found to be related to forest age, annual temperature, and precipitation at a global scale, but its determinants were different among various plant function types. The estimated global forest τ_w based on the filed data showed large spatial heterogeneity, which plays an important role in model simulation of AGB by a dynamic global vegetation model (DGVM). The τ_w could change the resulting AGB in tenfold based on a site-level test using the Monte Carlo method. At the global level, different parameterization schemes of the Integrated Biosphere Simulator using the estimated τ_w resulted in a twofold change in the AGB simulation for 2100. Our results highlight the influences of various biotic and abiotic variables on forest τ_w. The estimation of τ_w in our study may help improve the model simulations and reduce the parameter's uncertainty over the projection of future AGB in the current DGVM or Earth System Models. A clearer understanding of the responses of τ_w to climate change and the corresponding sophisticated description of forest growth/mortality in model structure is also needed for the improvement of carbon stock prediction in future studies.

1. Introduction

The large carbon flux between forest ecosystems and the atmosphere plays an essential role in the global carbon cycle [*Beer et al.*, 2010; *Xiao et al.*, 2011; *Xue et al.*, 2011, 2016]. This net carbon flux can be both determined by the rate of carbon assimilation (gross primary production (GPP)) and by the time of carbon being locked up in living plant tissue, i.e., woody residence time (τ_w, years) before being released into the atmosphere [*Lloyd and Farquhar*, 1996; *Malhi*, 2012]. The τ_w is an important physiological parameter that expresses the balance between forest recruitment/growth and mortality when it is in a steady condition [*Galbraith et al.*, 2013]. Many previous studies have found a close relationship between τ_w and forest carbon stocks and a large amount of uncertainty in the estimation of τ_w per se [*Vieira et al.*, 2005; *Zhou and Luo*, 2008; *Zhang et al.*, 2010; *Zhou et al.*, 2012]. Therefore, quantifying τ_w is important to gain a clearer understanding on the global forest carbon budget balance.

Dynamic global vegetation models (DGVMs) are useful tools for mapping global carbon stock and predicting its variation future. In most DGVMs, the global terrestrial ecosystems are represented by different plant functional types (PFTs), and much attention has been paid to improve the modeling of photosynthesis and GPP for each PFT. Typically, carbon stock or biomass has been simulated as the vegetation carbon pool including leaf, stem (including branch), and root produced from the allocation of net primary production (NPP). For forest ecosystems, the total aboveground biomass (AGB, Mg ha^{-1}) is mainly determined by the stem biomass. To predict forest growth and biomass accumulation, most DGVMs use the τ_w parameter to represent the time carbon remained in an ecosystem. The default PFT-specific value of τ_w introduces little spatial variance and is assumed to be temporally invariant for model simulation.

Although DGVMs could simulate biomass at regional to global scales, an increasing number of recent studies showed that the assumed invariant τ_w can induce large uncertainties in modeled biomass [*Delbart et al.*, 2010; *Castanho et al.*, 2013; *Friend et al.*, 2014]. *Friend et al.* [2014] explored the responses of the global vegetation to the projected climate by 2100 using seven global vegetation models (including DGVMs) and found large variations in global carbon stocks among these models. This large variation cannot be solely explained by the differences in simulated NPP; when uncertainties in τ_w were taken into account, an additional 30% of the variation was explained. In fact, trend of projected NPP were more consistent, while the temporal trend signs of τ_w may even be different (negative or positive) [*Friend et al.*, 2014]. These results demonstrated the necessity of accurately estimating τ_w during model simulations. A recent study based on forest field observations also showed that the spatial patterns of biomass of lowland Amazonian forests can be better explained by the patterns of τ_w rather than by the variation in forest productivity [*Malhi et al.*, 2015]. These authors stated that more attention should be paid to the allocation of NPP and τ_w aside from that for GPP [*Malhi et al.*, 2015]. However, the default values of τ_w for most current DGVMs are often not representative and may even be highly biased when compared with observed values [*Galbraith et al.*, 2013].

When forest is near equilibrium, biomass production can be balanced by biomass loss, and therefore, τ_w could be determined by forest mortality. At a regional or global scale, forest mortality may originate from either intrinsic self-thinning or natural and human disturbances, which makes it difficult to estimate τ_w [*Stephenson et al.*, 2011]. Previous studies have shown that τ_w could be closely related to abiotic (e.g., temperature and precipitation) or biotic (e.g., stand density) factors [*Lines et al.*, 2010; *Galbraith et al.*, 2013; *Malhi et al.*, 2015]. *Lines et al.* [2010] compiled forest mortality rates from forest inventory data and explored the influence of environmental and physiological variables for forests of the eastern United States. That study emphasized the influence of climate, soil, species, and size (stem diameter) on forest mortality rates at individual tree level. *Thurner et al.* [2016] estimated temperate and boreal forest residence time (including both aboveground and belowground forest carbon stocks) at the regional scale using remote sensing data. They found that the forest residence time was closely related to different climate drivers, depending on specific ecosystems. At the global scale, another term—carbon residence time (including both aboveground and belowground carbon stocks)—is used for all terrestrial ecosystems; researchers found that carbon residence time is highly correlated with temperature and precipitation [*Carvalhais et al.*, 2014]. More confidence in projected spatiotemporal variation in forest biomass would be achieved if more accurate τ_w or carbon residence time can be obtained by field observations or processes/empirical-based models.

The objective of this study is to investigate the determinants of forest τ_w based on field collected values and its role in the improvement of DGVM simulations. Specifically, we initially collected field-derived τ_w and analyzed the possible drivers of its change including environmental and biotic variables. Since global natural and anthropogenic disturbances are missing, we thus mainly focus on forest plots without disturbances for a long time. The collected field-derived τ_w covers all forest biomes including boreal, temperate, and tropical forests. Second, we generated a global, gridded τ_w map using the field-derived τ_w values and other meteorological and physiological variables as predictors with the random forest (RF) method. Third, we used the resulting global τ_w map to parameterize a DGVM–Integrated Biosphere Simulator (IBIS) [*Foley et al.*, 1996; *Kucharik et al.*, 2000], and based on an overview of different model descriptions of τ_w, we assessed how field-derived τ_w data can improve biomass simulations. Our results can improve our understanding of global patterns of τ_w and thus the global carbon cycle under climate change.

2. Materials and Methods

2.1. Collection of Woody Residence Time From Field Data

Assuming that forest is near an equilibrium state, τ_w can be calculated as follows [*Galbraith et al.*, 2013]:

$$\tau_w = \frac{\overline{M_w}}{\overline{W_p}} \tag{1}$$

where $\overline{M_w}$ is the mean AGB (Mg ha^{-1}) and $\overline{W_p}$ is the mean aboveground woody productivity (including stem and branch, Mg ha^{-1} yr^{-1}). Since we mainly focus on aboveground τ_w in the present study, AGB and aboveground $\overline{W_p}$ are used, which are different from *Thurner et al.* [2016]. For forest ecosystems, τ_w is closely related to, but not identical with, tree lifetime and is mainly determined by the lifetime of medium and large trees [*Galbraith et al.*, 2013; *Malhi et al.*, 2015].

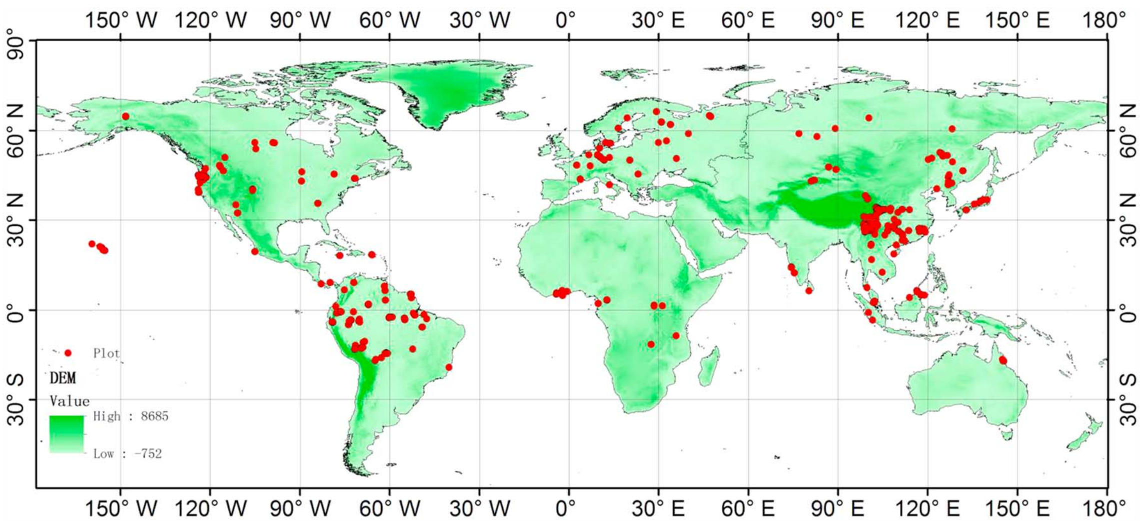

Figure 1. Spatial distribution of the 1319 forest sites where field calculated woody residence time (τ_w, years) data have been collected and used in the present study.

We compiled τ_w values for a total of 1319 forest sites from published literature. These sites cover all climate zones from boreal to temperate and tropical forests (Figure 1). To ensure the accuracy of our collected τ_w, we only collected data from sites with no major human or natural disturbances for at least 100 years. This was done to assure to a large extent that forest plots retained were near the equilibrium state. Similarly, only "mature" or "old growth" forests were selected in our analysis; that is, secondary forest sites that have not reached a state of equilibrium were excluded. For most of these sites, τ_w is not directly available, and we calculated τ_w from the reported AGB and woody productivity (including stem and branch) using equation (1).

Many of our τ_w values were obtained from four articles: *Galbraith et al.* [2013], *Luyssaert et al.* [2007], *Keeling and Phillips* [2007], and *Guo and Ren* [2014]. Most tropical forest sites are from *Galbraith et al.* [2013], who compiled the τ_w values for tropical forests from published literature. The τ_w values were calculated either by equation (1) or as the reciprocal of woody turnover time (see the supporting information of *Galbraith et al.* [2013] for details). *Luyssaert et al.* [2007] compiled aboveground biomass and NPP data for leaf, stem, and twig data for boreal, temperate, and tropical forests. We selected those forest sites that have historically lacked extensive human management for our analysis. *Keeling and Phillips* [2007] analyzed the relationship between forest productivity and aboveground biomass by compiling data from published literature. We calculated the τ_w values using their data set provided in the supporting information. *Guo and Ren* [2014] collected plot-level forest productivity and biomass data of natural and planted forests in China from published literature with detailed information on the forest carbon pools and other physiological characteristics of forests such as forest age, and we calculated the τ_w values for natural forests from the biomass and productivity data using equation (1). For each site, we also obtained meteorological data, i.e., annual precipitation (P, mm) and air temperature (T, °C) if these values were available in corresponding paper. For those sites where these variables were missing, we retrieved the values from global values of WorldClim (http://www.worldclim.org/).

2.2. Analysis of the Drivers of Woody Residence Time

We analyzed the global patterns of τ_w according to P and T. Further exploration of the relationships between τ_w and biotic variables of carbon use efficiency (CUE, ratio of NPP to GPP)/forest age was also conducted since these variables were considered to be closely related with $\overline{W_p}$ and AGB. Since not all of the plots contain information on forest age (938 plots) and GPP (32 plots) from in situ observations, fewer plots were used during this analysis. To examine how forest τ_w is determined by climate and forest age, we used linear mixed effect models (LMMs). The absolute values of soil nutrient contents were not available, and we thus assumed different random effects for local nutrient classification from Harmonized World Soil Database (http://webarchive.iiasa.ac.at/Research/LUC/External-World-soil-database/HTML/). We tested the effects of P, T, and forest age on τ_w by running all possible LMMs, which were evaluated by Akaike information criterion (AIC). Models with a $\Delta\text{AIC} \leq 7$ were selected for model averaging and coefficient estimation and then used to predict τ_w in relation to forest age, P, and T. Forest age and τ_w was log transformed as the nonlinear relationship between AGB and age. All explanatory variables were standardized by subtracting the mean from each value and dividing by the standard deviation to allow for easier interpretation of coefficients and improvement of model convergence [e.g., *Martin et al.*, 2016]. All LMM analyses are conducted by R with the nlme [*Pinheiro et al.*, 2015] and MuMIn [*Barton*, 2015] packages.

2.3. Estimation of Global Forest Woody Residence Time

In this study, to put τ_w as model parameter for a DGVM, i.e., Integrated Biosphere Simulator (IBIS), we extrapolated the field collected τ_w into spatial continuous layers by RF method [*Breiman*, 2001]. The RF method is a formalized nonparametric machine-learning algorithm and has been successfully used for parameter extrapolation [e.g., *Simard et al.*, 2011; *Su et al.*, 2016]. The main advantage of this method is that it does not require assumptions to be made regarding to the normality of covariables and can minimize the within-group variance. By the inherent unique tree "bagging" algorithm, the RF method can select a random subset of covariables at each candidate split and thus overcome the overfitting habit of decision tree algorithms [*Breiman*, 2001]. The RF extrapolation method was implemented based on the "randomForest" R package [*Liaw and Wiener*, 2002], which includes both classification and regression functions. We generated a regression "random forest" by the field collected τ_w and possible predictors. Two sets of global forest τ_w were generated: (1) present-day spatially variant τ_w and (2) projected spatially and temporally variant τ_w during 2006–2100 at the annual scale. Since we do not have the global wall-to-wall forest age and independent in situ woody NPP (and thus CUE), the predictors used in the RF method were different from those in the LMM analysis. The present-day τ_w was calculated by five ancillary predictors: T, P, GPP, evapotranspiration (ET), and digital elevation model (DEM). In contrast, three predictors, T, P, and DEM, were included to build the RF model and project annual τ_w by 2100. The global GPP/NPP and ET data sets were both available from the Numerical Terradynamic Simulation Group website (http://www.ntsg.umt.edu/biblio). The MOD17 GPP/NPP data sets were at a 1 km resolution on monthly (MOD17A2) and annual (MOD17A3) scales and are available from 2000 to the present year. The Moderate Resolution Imaging Spectroradiometer (MODIS) ET data set (MOD16) was produced by *Mu et al.* [2011], using a calculation algorithm based on the Penman-Monteith equation [*Monteith*, 1965] at a resolution of 1 km on a global scale. In our case, the improved version of annual MODIS ET products (MOD16A3) was used in the calculation, which was from a consistent version of meteorological variables from the Global Modeling and Assimilation Office, and this product has generally been validated and has acceptable accuracy [*Mu et al.*, 2011].The DEM data used were obtained from the NASA Shuttle Radar Topography Mission with a resolution of 1 km (http://srtm.csi.cgiar.org/). The projected spatially and temporally variant τ_w was calculated annually from the meteorological data from Community Climate System Model version 4.0 (CCSM4.0) simulated climatic variables under the Representative Concentration Pathway 4.5 (RCP4.5) scenario (http://www.cesm.ucar.edu/models/ccsm4.0/).

2.4. Model Description of Woody Residence Time

Most DGVMs simulate three carbon pools: leaves, stems (for trees), and roots [e.g., *Foley et al.*, 1996; *Sitch et al.*, 2003]. For a given PFT, an invariant value is commonly used for carbon residence time during model simulation. In IBIS, NPP is allocated among the three carbon pools at an annual scale. In steady state conditions, the instantaneous changes in the biomass pool j of PFT i are represented as

$$\frac{\partial C_{i,j}}{\partial t} = a_{i,j} NPP_i - \frac{C_{i,j}}{\tau_{i,j}} \tag{2}$$

where $a_{i,j}$ is the fraction of annual NPP allocated to the biomass pool and $\tau_{i,j}$ is the carbon residence time of that biomass pool, which is identical with τ_w for the carbon pool of stems and branches. Note that $a_{i,j}$ is a fixed value in IBIS; however, some other DGVMs (such as Lund-Potsdam-Jena [*Sitch et al.*, 2003]) estimate NPP allocation using allometric equations.

2.5. Model Simulation of AGB Using Estimated Woody Residence Time

We investigated how τ_w would improve the simulation of global forest AGB using IBIS. We first examined the influence of τ_w on simulated AGB at the site level using τ_w values ranging between 25th and 75th percentiles of each field-based PFT data. We then resampled the two global forest τ_w maps to a 0.5° × 0.5° scale to specify

Table 1. Candidate Mixed Effect Models for Explaining Global Forest Woody Residence Time (τ_w, Years)[a]

Models	Model Rank	Df	Log Likelihood	AIC	ΔAIC	Conditional R^2
A + T + P + A*T + A*P	1	8	−379.94	776.04	0	0.55
A + T + P + A*T + A*P + T*P	2	9	−379.7	777.59	1.55	0.55
A + T + P + A*P + T*P	3	8	−392.39	800.93	24.89	0.52
A + T + P + A*P	4	7	−393.53	801.18	25.14	0.52
A + P + A*P	5	6	−397.7	807.5	31.46	0.53
A + T + P + T*P	6	7	−416.67	847.46	71.42	0.5
A + T + P + A*T + T*P	7	8	−416.61	849.38	73.34	0.5
A + T + P	8	6	−421.67	855.44	79.4	0.5
A + T + P + A*T	9	7	−421.61	857.35	81.31	0.5
A + P	10	5	−431.46	872.98	96.94	0.51
A	11	4	−440.81	889.66	113.62	0.49
A + T	12	5	−439.87	889.8	113.76	0.49
A + T + A*T	13	6	−439.87	891.82	115.78	0.49
P	14	4	−671.52	1351.1	575.05	0.21
T + P	15	5	−670.61	1351.3	575.25	0.2
T + P + T*P	16	6	−670.53	1353.1	577.1	0.2
Null Model	17	3	−674.71	1355.4	579.4	0.21
T	18	4	−674.69	1357.4	581.38	0.2

[a]*A*: forest age, *T*: annual temperature, *P*: annual precipitation.

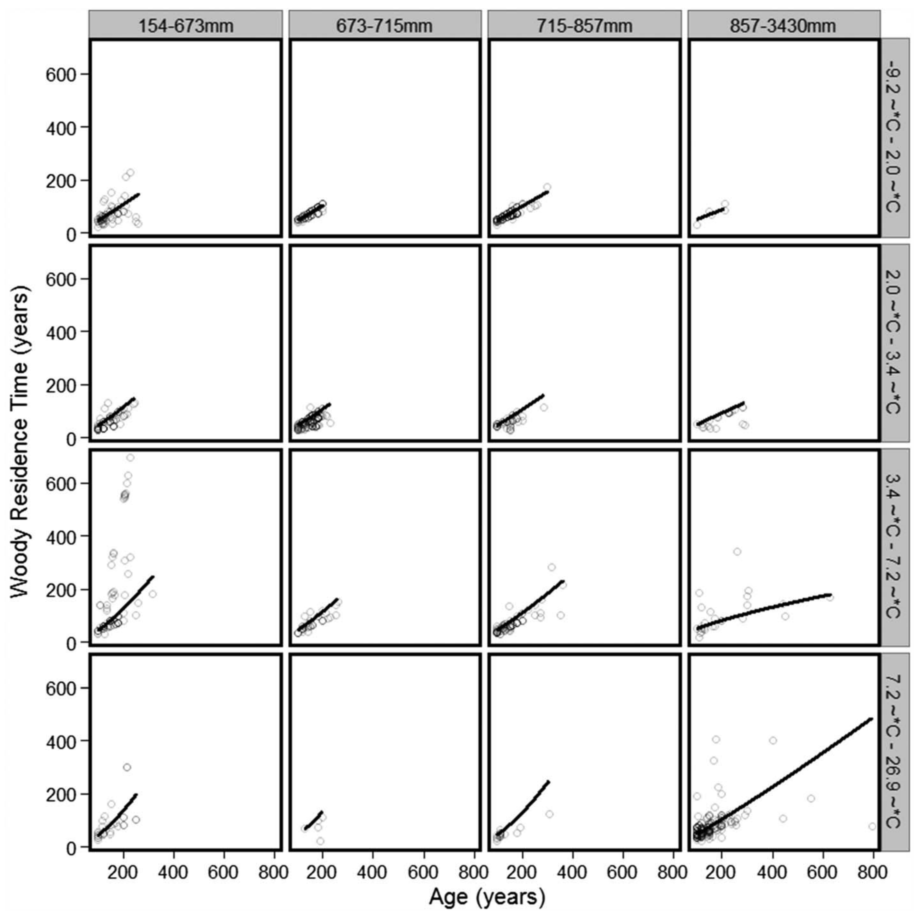

Figure 2. The relationship between forest age and τ_w for different climate zones. Panels represent binned mean annual temperature (rows) and total annual precipitation (columns). Each point represents an individual forest sites and the solid lines shows the predictions by model-averaged coefficients.

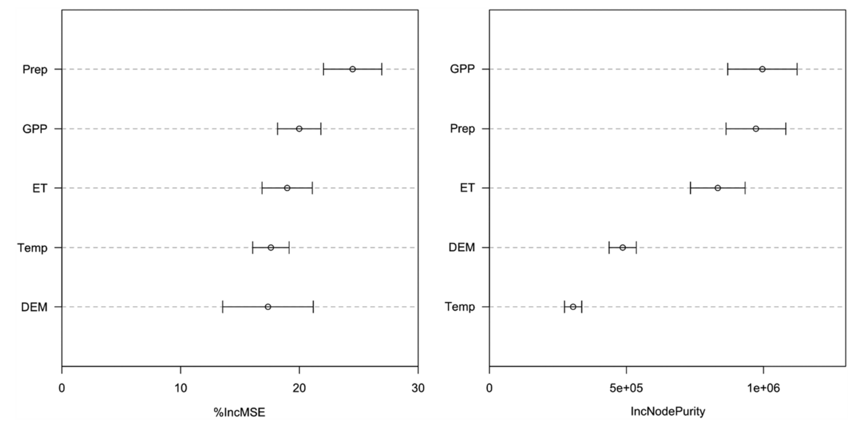

Figure 3. The mean importance of variables for 100 runs woody residency time random forest model, denoted by (a) the percentage increase of mean squared error (%IncMSE) and (b) the increase in node purity (IncNodePurity). Temp, Prep, GPP, ET, and DEM represent annual temperature, annual precipitation, gross primary production, evapotranspiration, and digital elevation model, respectively. %IncMSE means the percentage increase in mean squared error when the variable is randomized. IncNodePurity is a specific parameter for regression trees, which is measured by the residual sum of squares. The larger the %IncMSE and IncNodePurity of a variable are, the worse the model performs when the variable is randomized.

τ_w for IBIS model simulations. IBIS used the calculated τ_w for forests and default values for other PFTs (shrublands and grasses). In detail, we conducted three numerical experiments of global AGB simulations in 1948–2100 with different parameterization schemes: (1) parameterization with the temporally (and also spatially) dynamic τ_w (projected annual τ_w, only for 2006–2100), (2) parameterization with the spatially dynamic but temporally invariant τ_w (present-day τ_w), and (3) parameterization with the IBIS model default τ_w.

The climatic data to drive IBIS, including monthly mean air temperature, precipitation, relative humidity, cloudiness, diurnal temperature range, wind speed, and the number of wet days during 1948–2005 were obtained from the Climate Research Unit [*Harris et al.*, 2014]. These data were used as DGVM inputs to reproduce the amounts of global historical forest biomass during the years 1948–2005. Independent field collected forest AGB data (a total of 716 plots [*Hu et al.*, 2016]) with specific recorded measurement time were also compiled to validate the model simulations with improved and default τ_w (Figure S1 in the supporting information). To project the AGB to the end of 2100, the CCSM4.0 simulated climatic variables at the land surface under the RCP4.5 scenario (1.25° × 1.0°) were used to drive the DGVM. The CCSM4.0 data covering the period of 2006–2100 were downloaded and interpolated to a 0.5° × 0.5° resolution for model inputs.

3. Results

3.1. Drivers of Woody Residence Time

The model-averaged coefficients indicate positive relationships between τ_w and the logarithm of forest age (slope = 0.34 ± 0.01, importance value = 1, and $p < 0.001$) and mean annual temperature (slope = 0.07 ± 0.02, importance value = 1, and $p < 0.001$), which show negative relationship between mean annual precipitation (slope = -0.09 ± 0.02, importance value = 1, and $p < 0.001$). Furthermore, the slope related to forest age also increased (interaction term = -0.07 ± 0.01, importance value = 1, and $p < 0.001$) and decreased (interaction term = -0.1 ± 0.01, importance value = 1, and $p < 0.001$) with mean annual temperature and precipitation. The interaction term between temperature and precipitation is considered to be less important in characterizing forest τ_w (interaction term = 0.01 ± 0.01, importance value = 0.32, and $p = 0.48$). The first two models included in the model-averaging process have great prediction power (conditional $R^2 = 0.55$; Table 1 and Figure 2), and this results in an improved prediction performance compared with models containing only age, precipitation, or temperature (Table 1).

3.2. Estimation of Global Forest Woody Residence Time

The percentage increase in mean squared error (%IncMSE) and node purity (IncNodePurity) was calculated to evaluate the importance of each predictor (Figure 3). The absence of the annual precipitation and GPP will significantly increase mean squared error and node purity and thus lower the predictive ability of the RF

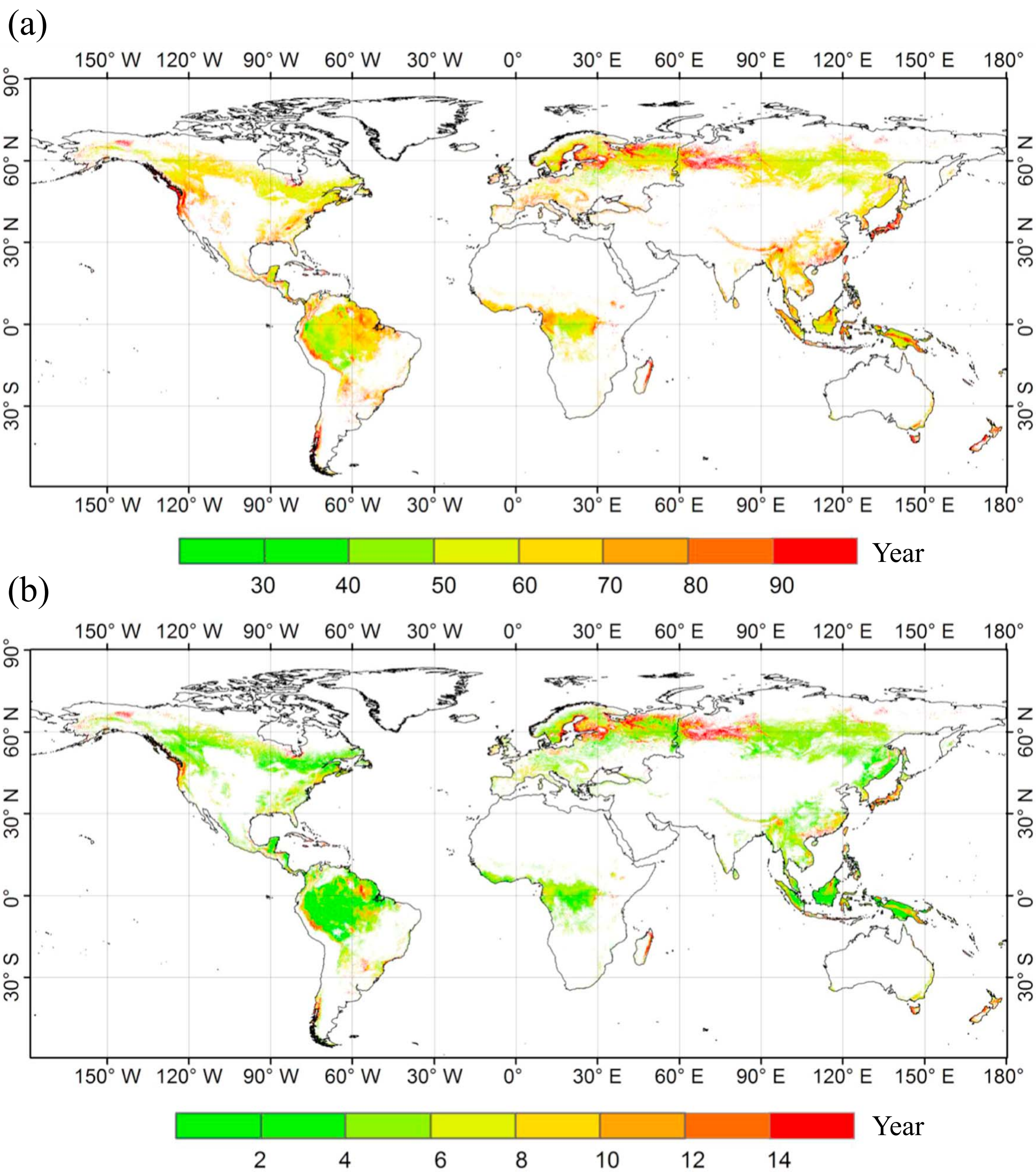

Figure 4. Spatial pattern of (a) the estimated woody residence time (τ_w, years) based on collected field data and (b) relative difference of estimated τ_w. The relative difference is estimated as the ratio of standard deviation of τ_w to the resulting τ_w. The standard deviation of τ_w is calculated when 75% of the collected field plot data were randomly selected in each of 100 random forest simulation model runs. The estimated τ_w has a 1 km resolution and was resampled to 0.5° × 0.5° when used as parameters for dynamic global vegetation model simulations in this study.

model. Therefore, these predictors are the two most important ones for the estimation of global τ_w. Similarly, ET, temperature, and DEM were also found to be effective predictors for the model.

The τ_w exhibits large spatial heterogeneity, with an average value of 66.7 years on a global scale (Figure 4). Large values of τ_w were found in tropical areas, especially in the Amazonian forests. The τ_w values in this area were generally above 50 years, and larger values above 70 years were observed in the eastern part of Amazonian forest, showing a west-east increasing gradient as highlighted by other authors [*Galbraith et al.*, 2013]. In contrast, τ_w for central African forests has a moderate value of about 50 years. The estimated τ_w for boreal forests in central Siberia also had a high value of greater than 100 years; meanwhile, the τ_w for

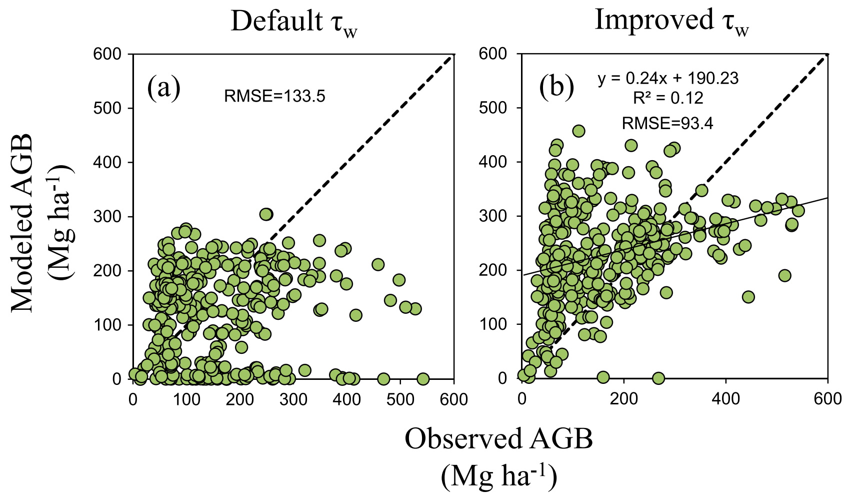

Figure 5. Comparison between observed and model-simulated aboveground biomass (AGB) by (a) default and (b) estimated present-day τ_w. Each point in the figure indicates the AGB measured in one or more plots (average for more than one plot) within a 0.5° × 0.5° model grid. Observed AGB was mostly measured during 1990–2010, and the model simulations were the averaged values during those corresponding years. The dashed line shows the 1:1 line. Root-mean-square error (Mg ha^{-1}) is also shown.

the Alaska forest had relatively high values greater than 60 years. European forests had a relatively high value of about 60 years in contrast with the temperate forests in other areas such as North America. However, the estimated values of τ_w are large (>100 years) for the temperate forests in the western areas of the United States. Similarly, the forests in subtropical areas of China and Japan also show large values. Areas with a large τ_w also exhibit a large degree of uncertainty such as areas in central and eastern Amazonia (Figure 4b).

3.3. Simulation of AGB Based on Estimated Woody Residence Time

Figure 5 shows the model performance of the simulated present-day AGB with model "default" and our estimated present-day τ_w. Each point in Figure 5 indicates one or more validation plots that are located in the same IBIS grid (0.5° × 0.5°). The simulated AGB using default τ_w showed large scattering, with underestimation for large amounts of AGB. Moreover, the default τ_w resulted in many small amounts of AGB (close to 0 Mg ha^{-1}), which indicates a nonforest PFT for the model simulation. The resulting AGB from the improved τ_w has a relatively close relationship with plot values, even though overestimation and underestimation were observed for small and large AGB values (Figure 5b). Note that the simulated AGB using our estimated present-day τ_w was also subjected to scattering, which may be caused by the scale difference between measured and simulated AGB (0.01° and 0.5°).

Ten Fluxnet sites, representing five different woody PFTs, were randomly selected to test the AGB uncertainties due to τ_w forward in time under RCP4.5 climate scenarios (Table S1 in the supporting information and Figure 6). The projected AGB was found to increase in most sites when using the averaged τ_w, but with large uncertainties caused by τ_w. One exception was observed for a boreal coniferous forest in Canada, where the AGB was consistently decreasing during all the test runs (Figure 6). The simulated AGB was shown to be sensitive to τ_w for all sites, resulting in a large variation in τ_w by the year of 2100. The projected AGB for Manaus and BANNA was found to increase fast when the averaged τ_w was used and a twofold AGB was obtained by 2100 for BANNA. The four temperate PFT sites witnessed similar simulation results and an increasing trend in AGB by 2100 for the averaged τ_w case, indicating that the temperate forests should benefit from the projected climate change in the future. Results from two of four boreal sites (US-WCr and US-Syr) revealed a generally constant AGB over the simulation period and a decreasing AGB for the remaining two of all τ_w cases. However, our simulation results also show that the boreal forest may benefit from future climate change with an increasing AGB trend in certain test cases. This further necessitates the accurate estimation of τ_w for model simulation.

10.1002/2016GB005557

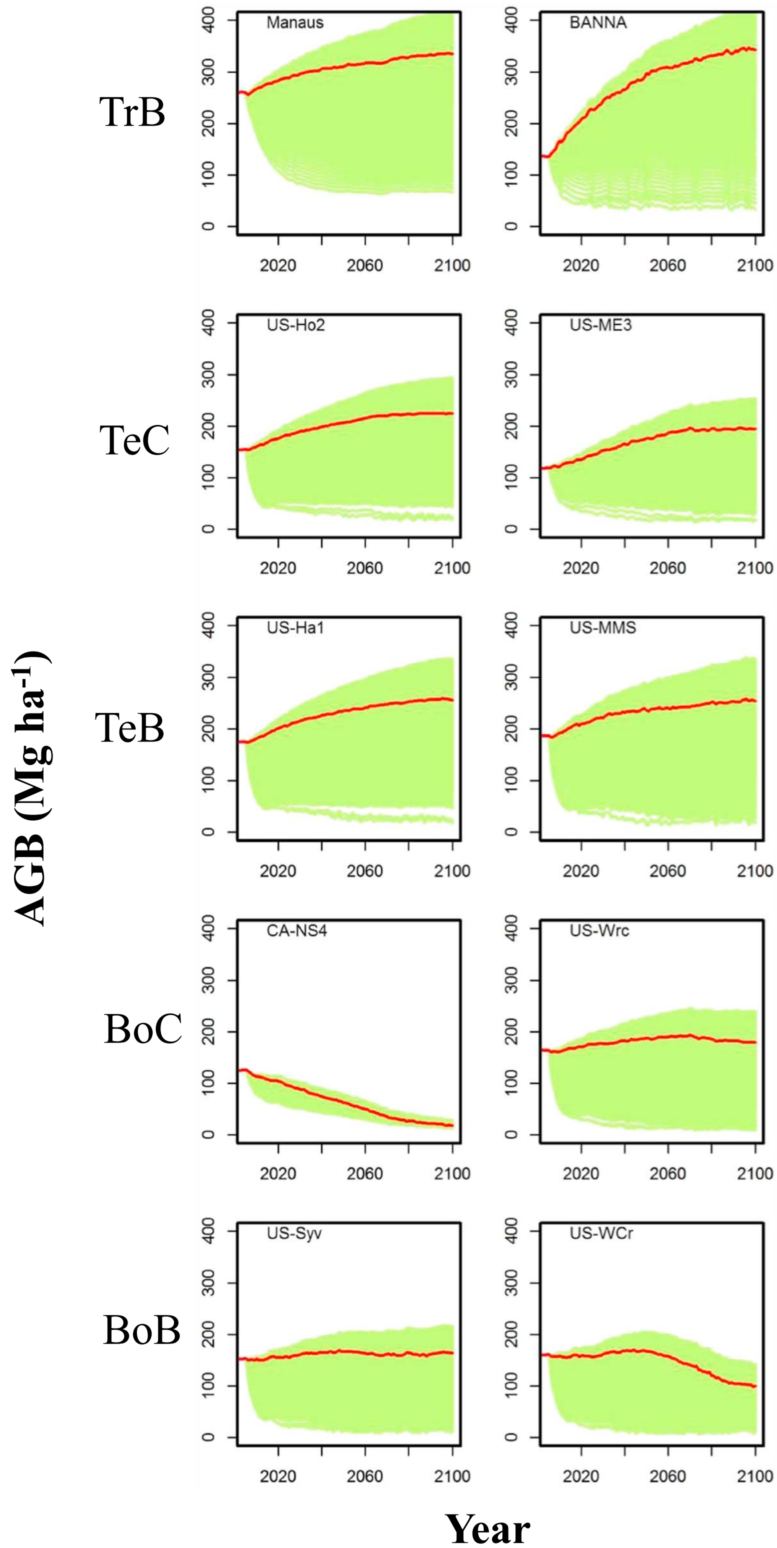

Figure 6. Simulated temporal trends of aboveground biomass during 2006–2100 for different plant functionaltTypes (PFTs) by the Integrated Biosphere Simulator (IBIS) under RCP4.5 scenario. The green lines show the 1000 test runs using the random τ_w data resulting between the one fourth and three fourth percentiles; the red line shows the result of the averaged τ_w based on the collected field data. The abbreviations are defined as follows: TrB, tropical broadleaf forest; TeC, temperate coniferous forest; TeB, temperate broadleaf forest; BoC, boreal coniferous forest; BoB, boreal broadleaf forest. All the test sites were randomly selected from Fluxnet; details of the sites are provided in Table S1.

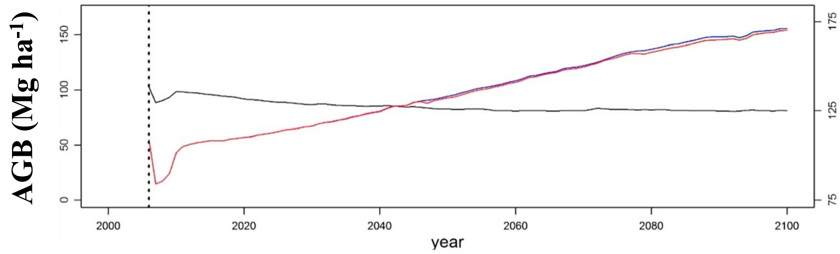

Figure 7. Temporal variations of the global average aboveground biomass (AGB, Mg ha^{-1}) simulated by the Integrated Biosphere Simulator during 2006–2100 under the RCP4.5 scenario for different parameterization schemes. Red line: parameterized by projected annual τ_w, blue line: present-day (adj) τ_w, black line: default τ_w.

Difference in the reproduced historical variations of AGB increased for the three model runs from 2006 to 2100 (Figure 7). The two improved runs with our estimated τ_w showed a consistent increasing trend for AGB, while the model run with default τ_w results in a decreasing trend and AGB does not change much after 2060. Though similar results were found for the two improved model runs, simulated AGB with present-day τ_w was slightly larger than that with projected annual τ_w. The simulated global forest AGB was 171.1 and 170.0 Mg ha^{-1} in 2100 for the two cases, respectively. Because the projected τ_w showed a decreasing trend by 2100 (Figure S2), assuming a constant τ_w may overestimate AGB for long-term simulations. Furthermore, the simulated spatial patterns of AGB in 2100 under the RCP4.5 scenario also showed large differences for the three runs (Figure S3). AGB from the two model runs with estimated τ_w is much larger in tropical forests and temperate forests areas compared with results with default τ_w. Another major difference was found for the transition from boreal coniferous evergreen forest to broadleaf cold deciduous forests in the Siberian areas, indicating the essential role of τ_w in mapping PFT over long-term simulation (Figure S4). Actually, the simulated forest PFT mapping showed large difference among the three simulation runs (Figure S4). Furthermore, the climate changes from cold and dry prior to 2040 to warm and wet later in the projected scenario. The interactions of changes in climate and the different woody residence values may result in the overall different variations in AGB for the simulation periods.

4. Discussion

4.1. Abiotic and Biotic Influences on Woody Residence Time

Few studies have focused on the mapping of τ_w at a global scale. A recent study investigated the global carbon residence time using field data and model simulations [*Carvalhais et al.*, 2014]. Because carbon residence time used in that study is different from τ_w in the present study in that the former calculates the residence time for both soil and vegetation residence time (including leaf, stem, and litter), comparing their values and our results directly would be difficult. However, their results show carbon residence time increases as temperature decreases in forests located in tropical to boreal areas, which is different from our results. This may be because decomposition occurs more slowly in boreal areas than in tropical areas because of the low temperature, resulting in the largest carbon residence time in boreal forests [*Carvalhais et al.*, 2014]. In our case, we did not consider soil carbon residence time and this could result in relatively small τ_w for boreal forests compared with other PFTs. This difference indicates that when calculating total ecosystem carbon stocks for both vegetation and soil, modelers should pay more attention to carbon residence time in soil of ecosystems in cold areas [*Yang et al.*, 2014; *Chen et al.*, 2015].

Globally, we observe a negative influence of *P* on τ_w according to LMM analysis; while *T* has positive influence on τ_w. However, the influence of *P* and *T* on τ_w may be different for a given PFT (Figure S5). *T* is found to be positively related to τ_w for boreal ($p = 0.54$) and temperate PFTs ($p < 0.05$), while it is negatively related to τ_w for warm temperate ($p = 0.63$) and tropical PFTs ($p < 0.05$). In cold areas, the forest may suffer from frost damage, thus resulting in large forest mortality [*Thurner et al.*, 2016]. Therefore, forest mortality in these areas is more controlled by temperature because of the inhibition of carbon assimilation for the low temperature and short grown season [*van Dijk et al.*, 2005; *Beer et al.*, 2010]. *Thurner et al.* [2016] found that the forest carbon residence time for temperate forests in Northern Hemisphere was more controlled by *P*, which is partly supported by our results (Figure S5). We found a quadratic relationship between *P* and τ_w for temperate forest. In detail, τ_w is found to decrease with *P* when *P* is below 1500 mm, while it increases with *P* when *P* is above 1500 mm. Most our collected temperate forest sites with *P* above 1500 mm are located in west North America with Mediterranean climate (Figure 1). The forests in these areas are found with large mortality in recent years most probably due to droughts [*van Mantgem and Stephenson*, 2007; *van Mantgem et al.*, 2009]. Even though the mechanism of forest mortality due to droughts is still controversial, drought-induced forest mortality has been widely observed globally [*Allen et al.*, 2015]. The temperate forest plots with *P* below 1500 mm are mostly located in coastal areas of Europe with high latitude and mountainous areas of China (Figure 1). Forest growth in these areas may be limited by the surplus water due to the limited evaporation [*Tao et al.*, 2016]. Thus, our results show that determinants of τ_w may be different even for the same PFT depending on the local climate [*Carvalhais et al.*, 2014; *Malhi et al.*, 2015; *Thurner et al.*, 2016]. Furthermore, several studies show that accumulation of woody biomass was more controlled by mortality due to extreme disturbance events instead of normal meteorological conditions [*Galbraith et al.*, 2013; *Thurner et al.*, 2016]. Therefore, the relationships using only *T* and *P* as predictors may not be enough for the global estimation of τ_w (Table 1 and Figure S6).

Our LMM analysis shows the important influence of interaction term between biotic term (i.e., age) and *T* (or *P*) on τ_w. Over large scales, τ_w may be determined more by forest structure and ecosystem succession [*Kobe et al.*, 1995; *Purves et al.*, 2008], climate [*Allen et al.*, 2015], and responses to climate change and disturbances [*Kurz et al.*, 2008]. Therefore, the estimation of forest mortality or τ_w, especially at a large scale, is difficult and also has large uncertainty [e.g., *Carvalhais et al.*, 2014; *Thurner et al.*, 2016]. *Malhi et al.* [2015] suggested that a direct link may exist between forest mortality (i.e., τ_w) and carbon use efficiency and/or woody allocation. Based on our collected sites available with CUE, we found inverse relationships between CUE and τ_w (Figure S6). Further analysis also shows a significant inverse relationship between woody allocation and τ_w for tropical forests ($n = 18$, data not shown). This indicates that the forests with a high CUE and $\overline{W_p}$ are usually characterized with a short life time, and therefore, AGB cannot be simply predicted by CUE or $\overline{W_p}$ [*Malhi et al.*, 2015]. The apparent relationship between high CUE and $\overline{W_p}$ with τ_w is not a direct result of variation in the productivity ($\overline{W_p}$); instead, they may be a result of forest ecosystem trade-offs between growth and defenses against large-scale disturbance such as wind or disease (along edaphic gradients) or perhaps reproduction and persistence (along climatic and edaphic gradients) by the surrogate of $\overline{W_p}$ [*Stephenson and van Mantgem*, 2005, 2011]. This has been partly verified in Amazonian forests, where an edaphic decreasing gradient exists from west to east [*Baker et al.*, 2004]. The eastern Amazonian forests growing on infertile soil (thus, with less subcanopy vegetation), more recourses are spent on forest defense while low productivity and slow growth favor a large τ_w; in contrast, the counterparts in western Amazonian forests on fertile soil (with more subcanopy) exhibit much higher productivity and rapid growth, which may result in a small τ_w (Figure 3b). Another research by *Quesada et al.* [2012] also shows that soil fertility plays an essential role in the dynamics of forest structure and biomass turnover in Amazonian forests by driving the patterns of mortality in the area.

4.2. Estimation of Global Forest Woody Residence Time

Based on the collected field data, we mapped the global woody residence time by a RF method (Figure 4). To our knowledge, this is the first τ_w map at the global scale, and therefore, this map may help improve model simulation of AGB by parameterizing τ_w using this data set (Figures 5 and 6). However, there is still uncertainty in the simulations (Figure 5b), which may originate from absence of plots in certainty areas (such as Siberia), the random forest method, and model structure in the description of forest growth/mortality. The LMM analysis shows the important influence of forest age and CUE on τ_w, while these two variables could not be integrated as predictors in the RF method because gridded forest age and CUE data at the global scale were not available yet. Therefore, large-scale estimation of these two variables should be to conducted in future to improve the calculation of τ_w in the RF method.

A recent research focusing on boreal and temperate forest residence time was published based on remote sensing data [*Thurner et al.*, 2016]. *Thurner et al.* [2016] calculated forest residence time for both above ground and below ground, and it is therefore difficult to compare their results with ours directly. Following the methods in *Thurner et al.* [2016], we downloaded AGB from *Thurner et al.* [2014] and also downloaded the global MODIS NPP and calculated τ_w for the boreal and temperate forests at 0.01° × 0.01° resolution

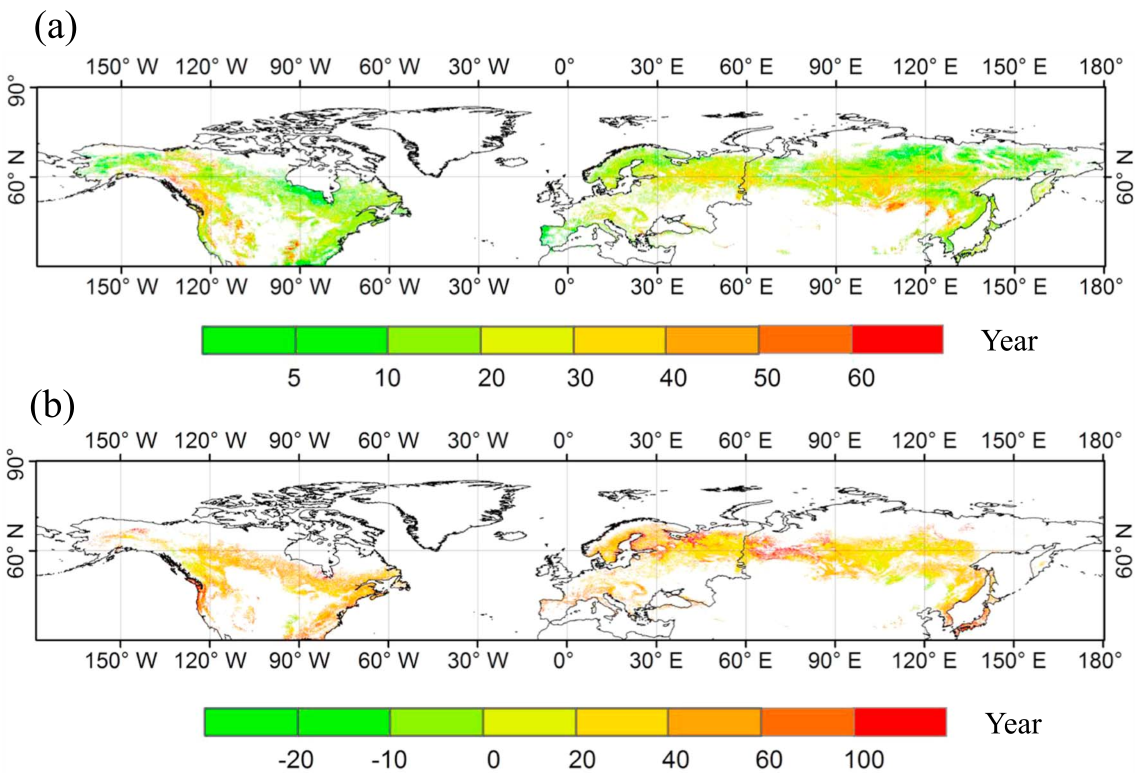

Figure 8. Spatial pattern of (a) estimated woody residence time (τ_w, years) according to the method from *Thurner et al.* [2016] and (b) difference between our estimate τ_w and results according to the method in *Thurner et al.* [2016]. Both of the τ_w maps have a resolution of 0.01° × 0.01°.

(Figures S7 and 8). Similar patterns were found for both of the two results, such as the relatively large values in Europe, northwestern United States, and Siberia (Figure 8). On the other hand, τ_w from our study is larger than that from *Thurner et al.* [2016] in most of the global forest areas (Figure 8b). This may be due to the fact that τ_w from our study was extrapolated from plot values assuming that forests were near equilibrium and the plots used for random forest calculation are largely undisturbed. Actually, secondary and/or human planted forests are found in North America and China and AGB for these forests were usually below equilibrium values [*Liu et al.*, 2014; *Galbraith et al.*, 2013]. We calculated τ_w based on their results by using a simple regression model to estimate aboveground NPP from MODIS NPP (Figure S8). This calculation processes may introduce uncertainty to the resulting τ_w and also make it difficult for the comparison. Nevertheless, with more remote sensing data of AGB and/or NPP becoming available for regional or global scale [e.g., *Thurner et al.*, 2014; *Hu et al.*, 2016], the method in *Thurner et al.* [2016] could have large potential in estimation of global forest τ_w.

4.3. Implications for Model Simulation

The τ_w can induce high levels of uncertainty in model simulation of AGB, both at site and global levels. This has already been shown in other model simulations as well as in field data-based analysis [*Delbart et al.*, 2010; *Castanho et al.*, 2013; *Friend et al.*, 2014; *Malhi et al.*, 2015]. Based on regional estimation of τ_w in Amazonian forests, *Castanho et al.* [2013] found that the spatially explicit τ_w could improve the accuracy of modeled AGB. Similarly, a large difference in estimated AGB was observed by different parameterization schemes of τ_w in our results (Figure 7).

DGVMs integrated in Earth system models (ESMs) are useful tools in the projection of future carbon fluxes and stocks at a global scale [e.g., *Friedlingstein et al.*, 2006; *Sitch et al.*, 2008]. Default values of τ_w for PFTs in DGVMs should be further calibrated based on additional field data (Table 2). Eight of 12 DGVMs use a fixed background turnover rate (or τ_w) and fire-induced mortality to simulate the overall τ_w. Even though some

Table 2. Default Woody Residence Time (τ_w, Years) in Different Dynamic Global Vegetation Model (DGVM)[a]

Model Name	General Approach	TrB	WTeB	WTeC	TeB	TeC	BoB	BoC	References
BIOME-BGC	Background turnover rate and fixed mortality rate	1.5	1.5	1.5	1.5	1.5	1.5	1.5	*Running and Coughlan* [1988]
CLM-DGVM	Simulated mortality rate due to negative carbon balance, competition, harsh climate, and fire	Dynamic values due to fire mortality							*Levis et al.* [2004]
HYBRID3.0	Fixed woody turnover rate	100	100	100	100	100	100	100	*Friend et al.* [1997]
ED2	Fixed mortality rate	250	250	250	250	333	250	333	*Medvigy et al.* [2009]
IBIS	Fixed woody biomass residence time	25	25	25	50	50	100	100	*Kucharik et al.* [2000]
JeDi-DGVM	Simulated dynamic woody biomass residence time	37							*Pavlick et al.* [2013]
JULES-TRIFFID	Fixed woody biomass residence time and disturbance rate	100	100	100	100	100	100	100	*Cox* [2001]
LPJ (origional)	Simulated mortality rate due to negative carbon balance, competition, harsh climate and fire	Dynamic values due to fire mortality							*Sitch et al.* [2003]
LPJ-GUESS	Background mortality rate and additional mortality rate due to harsh climate	Dynamic values due to mortality							*Smith et al.* [2001]
ORCHIDEE	Simulated mortality rate due to negative carbon balance, competition, harsh climate and fire	Dynamic values due to fire mortality							*Krinner et al.* [2005]
SEIB-DGVM	Simulated mortality rate due to forest growth and competition	20	20	20	20	20	20	20	*Sato et al.* [2007]
VISIT	Fixed woody turnover rate	15	20	20	20	20	500	500	*Ito and Oikawa* [2002]
Meta-analysis		64.1	104.1	72.0	82.9	74.7	55.5	80.9	This study

[a]The abbreviations are defined as follows: TrB, tropical broadleaf forest; WTeB, warm temperate broadleaf forest; WTeC, warm temperate coniferous forest; TeC, temperate coniferous forest; TeB, temperate broadleaf forest; BoC, boreal coniferous forest; BoB, boreal broadleaf forest.

models explicitly simulate mortality, these are still with uncertainty due to the unclear mechanisms in mortality per se [*McDowell et al.*, 2011]. No background τ_w is provided in Organizing Carbon and Hydrology in Dynamic Ecosystems (ORCHIDEE) and Community Land Model (CLM)-DGVM, and these two models explicitly simulate fire disturbance mortality modified from Lund-Potsdam-Jena (LPJ), which underestimates the mortality rate over a large scale. This results in overestimated τ_w and thus carbon stock, especially for tropical forests [*Krinner et al.*, 2005]. The Ecosystem Demography version 2 (ED2) model provides a density independent mortality rate for PFTs during different successional stages without providing an explicit background turnover rate. Only one of 12 models (i.e., Jena diversity (JeDi)-DGVM) investigated actually simulated the background τ_w using dynamic values; in this case it was determined by air temperature [*Pavlick et al.*, 2013]. The fixed background τ_w varies considerably even for the same PFT for the investigated models. For example, the τ_w for boreal coniferous forests ranges from 1.5 to 500 years for all the models; many default values are far from the averaged ones found in our meta-analysis. Furthermore, one third of the 12 models use the same values of τ_w for all PFTs in their simulations. This indicates that large variations of AGB may be derived in model simulations even with the same meteorological variables [*Sitch et al.*, 2008; *Friend et al.*, 2014]. Furthermore, most of the current DGVMs only consider background mortality and influences of natural disturbances on τ_w and do not explicitly simulate human disturbances. Further uncertainties in AGB may also arise from assumptions of the homogeneity of forest stands (such as equal probability of forest mortality for all species) and the steady state in the DGVM calculations. Therefore, even though our estimated gridded τ_w may help in the parameterization of models at this stage, more work should be done to explore the forest mortality mechanisms in the future [*McDowell et al.*, 2011] and thus to improve model structure in the description of recruitment and mortality.

Several studies observed the lessened τ_w during the most recent decades [*Phillips and Gentry*, 1994; *Phillips et al.*, 2004], which is different from the fixed temporal τ_w in models (Figure S2). The change in τ_w was, to a large extent, caused by climate change such as the warming temperature and/or the increasing atmospheric CO_2 concentration [*Phillips and Gentry*, 1994; *Phillips et al.*, 2004]. The ESMs projected enhanced forest productivity in the current century mainly caused by global warming and CO_2 fertilization [e.g., *Cramer et al.*, 2001; *Sitch et al.*, 2008; *Piao et al.*, 2013]. Therefore, an invariant τ_w may result in an overestimation of simulated AGB according to equation (1) if τ_w decreased in the future. Our simulation results show that assuming a time invariant τ_w may result in larger AGB compared with using the projected τ_w (Figures 7 and S3). Therefore, a better understanding and prediction on the responses of τ_w to climate change and atmospheric CO_2 concentration is needed and should be fully investigated.

5. Conclusions

The τ_w is an important parameter that expresses the balances between mature forest recruitment/growth and mortality. By collecting field data from the literature, this study explores the global forest woody residence time and investigates its influences on model simulations of AGB at the global scale. Parameter τ_w is highly related with forest age, *T* and *P*, but shows different determinants among various PFTs. The estimated global forest τ_w based on the collected field data shows large spatial heterogeneity as well. This heterogeneity plays an important role in model simulation of carbon stocks in DGVMs. Parameter τ_w could change the resulted AGB in 10 folds based on a site-level test using the Monte Carlo method. At the global level, different parameterization schemes of the Integrated Biosphere Simulator using estimated τ_w resulted in a twofold change in AGB for 2100. The results from the study highlight the influences by various biotic and abiotic variables on forest τ_w. The global estimation of τ_w may help improve the model simulations and lower the parameter uncertainty over the projection of future AGB in current DGVM or ESM models. A clearer understanding of τ_w responses to climate change is also needed for the improvement of model prediction of carbon stock in future studies.

Acknowledgments
The National Natural Science Foundation of China (grant 41301020) and the National Key Basic Research Program of China (grant 2013CB956604) supported this study financially. Jingfeng Xiao was supported by the National Aeronautics and Space Administration (NASA) through the Carbon Cycle Science Program (grant NNX14AJ18G) and Climate Indicators and Data Products for Future National Climate Assessments (grant NNX16AG61G). The authors express their sincere thanks to graduate students from the Digital Ecosystem Lab of Institute of Botany, Chinese Academy of Sciences, for assistance with the data analysis. All data used and RF model results can be accessed at http://www.guolablidar.com/. We thank the Editor and anonymous reviewers for their valuable comments on the manuscript.

References

Allen, C. D., D. D. Breshears, and N. G. McDowell (2015), On underestimation of global vulnerability to tree mortality and forest die-off from hotter drought in the Anthropocene, *Ecosphere*, *6*, 129.

Baker, T. R., et al. (2004), Variation in wood density determines spatial patterns in Amazonian forest biomass, *Global Change Biol.*, *10*, 545–562.

Barton K. (2015), MuMIn: Multi-model inference. Version 1.15.6. [Available at https://cran.r-project.org/web/packages/MuMIn/index.html.]

Beer, C., et al. (2010), Terrestrial Gross carbon dioxide uptake: Global distribution and covariation with climate, *Science*, *329*, 834–838.

Breiman, L. (2001), Random forests, *Mach. Learn.*, *45*, 5–32.

Carvalhais, N., et al. (2014), Global covariation of carbon turnover times with climate in terrestrial ecosystems, *Nature*, *514*, 213–217.

Castanho, A. D. A., M. T. Coe, M. H. Costa, Y. Malhi, D. Galbraith, and C. A. Quesada (2013), Improving simulated Amazon forest biomass and productivity by including spatial variation in biophysical parameters, *Biogeosciences*, *10*, 2255–2272.

Chen, L., P. Smith, and Y. Yang (2015), How has soil carbon stock changed over recent decades?, *Global Change Biol.*, *21*, 3197–3199.

Cramer, W., et al. (2001), Global response of terrestrial ecosystem structure and function to CO_2 and climate change: Results from six dynamic global vegetation models, *Global Change Biol.*, *7*, 357–373.

Cox, P. M. (2001), Description of the "TRIFFID" dynamic global vegetation model, *Hadley Centre Tech. Note 24*.

Delbart, N., P. Ciais, J. Chave, N. Viovy, Y. Malhi, and T. Le Toan (2010), Mortality as a key driver of the spatial distribution of aboveground biomass in Amazonian forest: Results from a dynamic vegetation model, *Biogeosciences*, *7*, 3027–3039.

Foley, J. A., I. C. Prentice, N. Ramankutty, S. Levis, D. Pollard, S. Sitch, and A. Haxeltine (1996), An integrated biosphere model of land surface processes, terrestrial carbon balance, and vegetation dynamics, *Global Biogeochem. Cycles*, *10*, 603–628, doi:10.1029/96GB02692.

Friedlingstein, P., et al. (2006), Climate-carbon cycle feedback analysis: Results from the (CMIP)-M-4 model intercomparison, *J. Clim.*, *19*, 3337–3353.

Friend, A. D., A. K. Stevens, R. G. Knox, and M. G. R. Cannell (1997), A process-based, terrestrial biosphere model of ecosystem dynamics (hybrid v3.0), *Ecol. Model.*, *95*, 249–287.

Friend, A. D., et al. (2014), Carbon residence time dominates uncertainty in terrestrial vegetation responses to future climate and atmospheric CO_2, *Proc. Natl. Acad. Sci.*, *111*, 3280–3285.

Galbraith, D., et al. (2013), Residence times of woody biomass in tropical forests, *Plant Ecol. Diver.*, *6*, 139–157.

Guo, Q., and H. Ren (2014), Productivity as related to diversity and age in planted versus natural forests, *Glob. Ecol. Biogeogr.*, *23*, 1461–1471.

Harris, I., P. D. Jones, T. J. Osborn, and D. H. Lister (2014), Updated high-resolution grids of monthly climatic observations—The CRU TS3.10 dataset, *Int. J. Climatol.*, *34*, 623–642.

Hu, T., Y. Su, B. Xue, J. Liu, X. Zhao, J. Fang, and Q. Guo (2016), Mapping global forest aboveground biomass with spaceborne LiDAR, optical imagery, and forest inventory data, *Remote Sens.*, *8*, 565, doi:10.3390/rs8070565.

Ito, A., and T. Oikawa (2002), A simulation model of the carbon cycle in land ecosystems (Sim-CYCLE): A description based on dry-matter production theory and plot-scale validation, *Ecol. Model.*, *151*, 143–176.

Keeling, H. C., and O. L. Phillips (2007), The global relationship between forest productivity and biomass, *Glob. Ecol. Biogeogr.*, *16*, 618–631.

Kobe, R. K., S. W. Pacala, J. A. Silander, and C. D. Canham (1995), Juvenile tree survivorship as a component of shade tolerance, *Ecol. Appl.*, *5*, 517–532.

Krinner, G., N. Viovy, N. de Noblet-Ducoudré, J. Ogée, J. Polcher, P. Friedlingstein, P. Ciais, S. Sitch, and I. C. Prentice (2005), A dynamic global vegetation model for studies of the coupled atmosphere-biosphere system, *Global Biogeochem. Cycles*, *19*, GB1015, doi:10.1029/2003GB002199.

Kucharik, C. J., J. A. Foley, C. Delire, V. A. Fisher, M. T. Coe, J. D. Lenters, C. Young-Molling, N. Ramankutty, J. M. Norman, and S. T. Gower (2000), Testing the performance of a dynamic global ecosystem model: Water balance, carbon balance, and vegetation structure, *Global Biogeochem. Cycles*, *14*, 795–825, doi:10.1029/1999GB001138.

Kurz, W. A., C. C. Dymond, G. Stinson, G. J. Rampley, E. T. Neilson, A. L. Carroll, T. Ebata, and L. Safranyik (2008), Mountain pine beetle and forest carbon feedback to climate change, *Nature*, *452*, 987–990.

Levis, S., G. B. Bonan, M. Vertenstein, and K. W. Oleson (2004), The Community Land Model's Dynamic Global Vegetation Model (CLMDGVM): Technical description and user's guide, 50 pp., *NCAR Tech. Note NCAR/TN-459+IA*, Natl. Cent. for Atmos. Res., Boulder, Colo.

Liaw, A., and M. Wiener (2002), Classification and regression by random Forest, *R News*, *2*, 18–22.

Lines, E. R., D. A. Coomes, and D. W. Purves (2010), Influences of Forest structure, climate and species composition on tree mortality across the eastern US, *PLoS One*, *5*, e13212.

Liu, D., Y. Chen, W. Cai, W. Dong, J. Xiao, J. Chen, H. Zhang, J. Xia, and W. Yuan (2014), The contribution of China's Grain to Green Program to carbon sequestration, *Landsc. Ecol.*, *29*, 1675–1688.

Lloyd, J., and G. D. Farquhar (1996), The CO_2 dependence of photosynthesis, plant growth responses to elevated atmospheric CO_2 concentrations and their interaction with soil nutrient status. I. General principles and forest ecosystems, *Funct. Ecol.*, *10*, 4–32.

Luyssaert, S., et al. (2007), CO_2 balance of boreal, temperate, and tropical forests derived from a global database, *Global Change Biol.*, *13*, 2509–2537.

Malhi, Y. (2012), The productivity, metabolism and carbon cycle of tropical forest vegetation, *J. Ecol.*, *100*, 65–75.

Malhi, Y., et al. (2015), The linkages between photosynthesis, productivity, growth and biomass in lowland Amazonian forests, *Global Change Biol.*, *21*, 2283–2295.

Martin, P., M. Jung, F. Q. Brearley, R. R. Ribbons, E. R. Lines, and A. L. Jacob (2016), Can we set a global threshold age to define mature forests?, *Peer J.*, *4*, e1595.

McDowell, N. G., D. J. Beerling, D. D. Breshears, R. A. Fisher, K. F. Raffa, and M. Stitt (2011), The interdependence of mechanisms underlying climate-driven vegetation mortality, *Trends Ecol. Evol.*, *26*, 523–532.

Medvigy, D., S. C. Wofsy, J. W. Munger, D. Y. Hollinger, and P. R. Moorcroft (2009), Mechanistic scaling of ecosystem function and dynamics in space and time: Ecosystem Demography model version 2, *J. Geophys. Res.*, *114*, G01002, doi:10.1029/2008JG000812.

Monteith, J. L. (1965), Evaporation and the Environment, in *19th Symposia of the Society for Experimental Biology*, vol. 19, pp. 205–235.

Mu, Q., M. Zhao, and S. W. Running (2011), Improvements to a MODIS global terrestrial evapotranspiration algorithm, *Remote Sens. Environ.*, *115*, 1781–1800.

Pavlick, R., D. T. Drewry, K. Bohn, B. Reu, and A. Kleidon (2013), The Jena diversity-dynamic global vegetation model (JeDi-DGVM): A diverse approach to representing terrestrial biogeography and biogeochemistry based on plant functional trade-offs, *Biogeosciences*, *10*, 4137–4177.

Phillips, O. L., and A. H. Gentry (1994), Increasing turnover through time in tropical forests, *Science*, *263*, 954–958.

Phillips, O. L., et al. (2004), Pattern and process in Amazon tree turnover, 1976–2001, *Philos. Trans. R. Soc. Lond. B: Biol. Sci.*, *359*, 381–407.

Piao, S., et al. (2013), Evaluation of terrestrial carbon cycle models for their response to climate variability and to CO_2 trends, *Global Change Biol.*, *19*, 2117–2132.

Pinheiro, J., D. Bates, S. DebRoy, D. Sarkar, and R Core Team (2015), Nlme: Linear and nonlinear mixed effects models. R package version 3.1-120. [Available at http://CRAN.R-project.org/package=nlme.]

Purves, D. W., J. W. Lichstein, N. Strigul, and S. W. Pacala (2008), Predicting and understanding forest dynamics using a simple tractable model, *Proc. Natl. Acad. Sci.*, *105*, 17,018–17,022.

Quesada, C. A., et al. (2012), Basin-wide variations in Amazon forest structure and function are mediated by both soils and climate, *Biogeosciences*, *9*, 2203–2246.

Running, S. W., and J. C. Coughlan (1988), A general model of forest ecosystem processes for regional applications I. Hydrologic balance, canopy gas exchange and primary production processes, *Ecol. Model.*, *42*, 125–154.

Sato, H., A. Itoh, and T. Kohyama (2007), SEIB–DGVM: A new dynamic global vegetation model using a spatially explicit individual-based approach, *Ecol. Model.*, *200*, 279–307.

Simard, M., N. Pinto, J. B. Fisher, and A. Baccini (2011), Mapping forest canopy height globally with spaceborne lidar, *J. Geophys. Res.*, *116*, G04021, doi:10.1029/2011JG001708.

Sitch, S., et al. (2003), Evaluation of ecosystem dynamics, plant geography and terrestrial carbon cycling in the LPJ dynamic global vegetation model, *Global Change Biol.*, *9*, 161–185.

Sitch, S., et al. (2008), Evaluation of the terrestrial carbon cycle, future plant geography and climate-carbon cycle feedbacks using five dynamic global vegetation models (DGVMs), *Global Change Biol.*, *14*, 2015–2039.

Smith, B., I. C. Prentice, and M. T. Sykes (2001), Representation of vegetation dynamics in the modelling of terrestrial ecosystems: Comparing two contrasting approaches within European climate space, *Global Ecol. Biogeogr.*, *10*, 621–637.

Stephenson, N. L., and P. J. van Mantgem (2005), Forest turnover rates follow global and regional patterns of productivity, *Ecol. Lett.*, *8*, 524–531.

Stephenson, N. L., P. J. van Mantgem, A. G. Bunn, H. Bruner, M. E. Harmon, K. B. O'Connell, D. L. Urban, and J. F. Franklin (2011), Causes and implications of the correlation between forest productivity and tree mortality rates, *Ecol. Monogr.*, *81*, 527–555.

Su, Y., Q. Guo, B. Xue, T. Hu, O. Alvarez, S. Tao, and J. Fang (2016), Spatial distribution of forest aboveground biomass in China: Estimation through combination of spaceborne lidar, optical imagery, and forest inventory data, *Remote Sens. Environ.*, *173*, 187–199.

Tao, S., Q. Guo, C. Li, Z. Wang, and J. Fang (2016), Global patterns and determinants of forest canopy height, *Ecology*, *97*, 3265–3270.

Thurner, M., et al. (2014), Carbon stock and density of northern boreal and temperate forests, *Global Ecol. Biogeogr.*, *23*, 297–310.

Thurner, M., C. Beer, N. Carvalhais, M. Forkel, M. Santoro, M. Tum, and C. Schmullius (2016), Large-scale variation in boreal and temperate forest carbon turnover rate related to climate, *Geophys. Res. Lett.*, *43*, 4576–4585, doi:10.1002/2016GL068794.

van Dijk, A., A. J. Dolman, and E. D. Schulze (2005), Radiation, temperature, and leaf area explain ecosystem carbon fluxes in boreal and temperate European forests, *Global Biogeochem. Cycles*, *19*, GB2029, doi:10.1029/2004GB002417.

van Mantgem, P. J., and N. L. Stephenson (2007), Apparent climatically induced increase of tree mortality rates in a temperate forest, *Ecol. Lett.*, *10*, 909–916.

van Mantgem, P. J., et al. (2009), Widespread increase of tree mortality rates in the western United States, *Science*, *323*, 521–524.

Vieira, S., S. Trumbore, P. B. Camargo, D. Selhorst, J. Q. Chambers, N. Higuchi, and L. A. Martinelli (2005), Slow growth rates of Amazonian trees: Consequences for carbon cycling, *Proc. Natl. Acad. Sci. U.S.A.*, *102*, 18,502–18,507.

Xiao, J., et al. (2011), Assessing net ecosystem carbon exchange of U.S. terrestrial ecosystems by integrating eddy covariance flux measurements and satellite observations, *Agric. For. Meteorol.*, *151*, 60–69.

Xue, B.-L., T. O. Kumagai, S. I. Iida, T. Nakai, K. Matsumoto, H. Komatsu, K. Otsuki, and T. Ohta (2011), Influences of canopy structure and physiological traits on flux partitioning between understory and overstory in an eastern Siberian boreal larch forest, *Ecol. Model.*, *222*, 1479–1490.

Xue, B.-L., Q. Guo, Y. Gong, T. Hu, J. Liu, and T. Ohta (2016), The influence of meteorology and phenology on net ecosystem exchange in an eastern Siberian boreal larch forest, *J. Plant Ecol.*, *9*, 520–530.

Yang, Y., P. Li, J. Ding, X. Zhao, W. Ma, C. Ji, and J. Fang (2014), Increased topsoil carbon stock across China's forests, *Global Change Biol.*, *20*, 2687–2696.

Zhang, L., Y. Luo, G. Yu, and L. Zhang (2010), Estimated carbon residence times in three forest ecosystems of eastern China: Applications of probabilistic inversion, *J. Geophys. Res.*, 115, G01010, doi:10.1029/2009JG001004.

Zhou, T., and Y. Luo (2008), Spatial patterns of ecosystem carbon residence time and NPP-driven carbon uptake in the conterminous United States, *Global Biogeochem. Cycles*, *22*, GB3032, doi:10.1029/2007GB002939.

Zhou, X., T. Zhou, and Y. Luo (2012), Uncertainties in carbon residence time and NPP-driven carbon uptake in terrestrial ecosystems of the conterminous USA: A Bayesian approach, *Tellus Ser. B-Chem. Phys. Meteorol.*, *64*.